JACS
JOURNAL OF THE AMERICAN CHEMICAL SOCIETY
Communication
pubs.acs.org/JACS

Integration of Gold Nanoparticles into Bilayer Structures via Adaptive Surface Chemistry

Hee-Young Lee,[†] Sun Hae Ra Shin,[†] Ludmila L. Abezgauz,[‡] Sean A. Lewis,[†] Aaron M. Chirsan,[†] Dganit D. Danino,[‡] and Kyle J. M. Bishop*[,†]

[†]Department of Chemical Engineering, The Pennsylvania State University, University Park, Pennsylvania 16803, United States
[‡]Department of Biotechnology and Food Engineering, Technion, Haifa 32000, Israel

Supporting Information

ABSTRACT: We describe the spontaneous incorporation of amphiphilic gold nanoparticles (Au NPs) into the walls of surfactant vesicles. Au NPs were functionalized with mixed monolayers of hydrophilic (deprotonated mercaptoundecanoic acid, MUA) and hydrophobic (octadecanethiol, ODT) ligands, which are known to redistribute dynamically on the NP surface in response to changes in the local environment. When Au NPs are mixed with preformed surfactant vesicles, the hydrophobic ODT ligands on the NP surface interact favorably with the hydrophobic core of the bilayer structure and guide the incorporation of NPs into the vesicle walls. Unlike previous strategies based on small hydrophobic NPs, the present approach allows for the incorporation of water-soluble particles even when the size of the particles greatly exceeds the bilayer thickness. The strategy described here based on inorganic NPs functionalized with two labile ligands should in principle be applicable to other nanoparticle materials and bilayer structures.

The incorporation of inorganic nanoparticles (NPs) into lipid bilayers has important implications for medical imaging,[1] phototherapy treatments,[2] and nanoparticle-actuated vesicles[3−6] for controlled drug release. Depending on the material, the nanoparticle core imparts desirable functionalities such as enhanced fluorescence,[1,7] plasmonic excitation,[8] or magnetic actuation.[3,4] The magnitude of these effects scales strongly with the particle diameter (D). For example, the absorption cross sections for both quantum dots[9] and plasmonic NPs[8] scale as D^3, as do the dipole moments of magnetic particles.[10] Consequently, it is often desirable to use larger particles with dimensions exceeding the thickness of lipid bilayers (typically, ∼4 nm[11]). Existing methods[1,3,12,13] for incorporating NPs into bilayer structures are limited to small particles functionalized with hydrophobic surfaces that "fit" within the hydrophobic core of the membrane. Larger particles[1,3] do not fuse with lipid bilayers but rather form lipid-covered NP micelles[14] as explained by thermodynamic models.[15,16] Regardless of their size, hydrophobic particles are also difficult to incorporate into preformed aqueous vesicles (or living cells) without the use of stabilizing detergents that must subsequently be removed.[12]

By contrast, NPs functionalized with mixed monolayers containing both hydrophobic and hydrophilic ligands have been shown to penetrate the cell membrane and still dissolve easily in water.[17] Such particles have the interesting ability to adapt their surface chemistry in response to environmental cues, as further evidenced by the formation of amphiphilic, Janus-type NPs at liquid interfaces.[18,19] Recent theoretical results[20] suggest that such environmentally responsive particles containing binary mixtures of mobile ligands—one hydrophobic, one hydrophilic—can penetrate and fuse with lipid bilayers even when the particle dimensions greatly exceed that of the membrane.

Here we confirm this prediction experimentally and demonstrate that relatively large (∼6 nm in diameter) gold NPs functionalized with mixed monolayers of hydrophobic octadecanethiol (ODT) and hydrophilic mercaptoundecanoic acid (MUA) are spontaneously incorporated into the walls of surfactant vesicles (∼2.5 nm thick[21,22]). The formation of NP−vesicle structures is achieved simply by mixing amphiphilic Au NPs and preformed surfactant vesicles in aqueous solution (Figure 1). The hydrophobic ODT ligands on the NP surface interact favorably with the hydrophobic core of the bilayer structure to guide the incorporation of the NPs into the vesicle walls. Furthermore, as the NPs and the vesicles are negatively charged, the formation of NP−vesicle structures can be controlled by varying the salt concentration in solution.

Initially, as-prepared[23,24] Au NPs (6.2 ± 0.8 nm in diameter) were stabilized by weakly bound dodecylamine (DDA) ligands and dispersed in toluene. The surface of the AuDDA NPs was subsequently functionalized with mixed monolayers of MUA and ODT via ligand exchange [see section 1 in the Supporting Information (SI)]. The resulting AuMUA/ODT NPs were washed to remove excess ligands and dispersed in deionized water with the pH adjusted to >11 by addition of tetramethylammonium hydroxide (TMAOH) to deprotonate the MUA ligands fully.[25]

The ODT:MUA ratio (χ = 8) was chosen to be as large as possible to yield water-soluble particles that interact strongly with the hydrophobic core of the surfactant bilayers. As this ratio differs from that on the surface of the particles (χ_{surf}), the latter was determined independently via electrostatic titrations[26] of the negatively charged NPs with the cationic surfactant cetyltrimethylammonium tosylate (CTAT) (Figure 2a). Dropwise addition of 1 mM CTAT solution to a 2 mM

Received: January 8, 2013
Published: April 5, 2013

   dx.doi.org/10.1021/ja400225n | J. Am. Chem. Soc. 2013, 135, 5950−5953

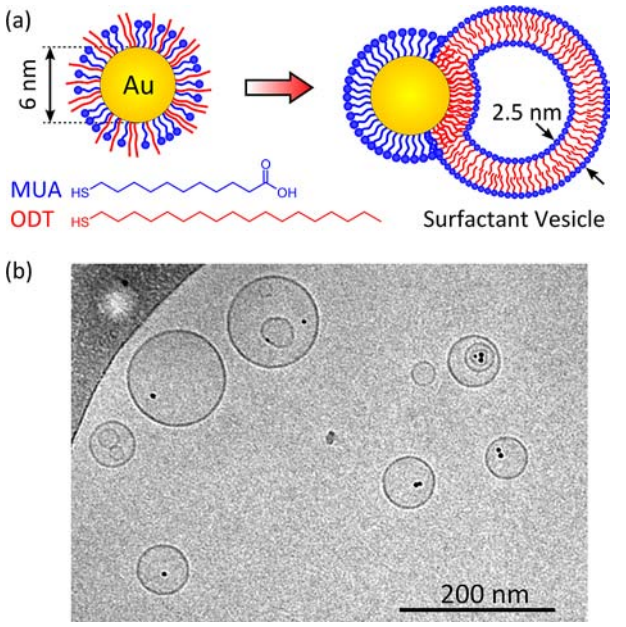

Figure 1. (a) Au NPs functionalized with mixed monolayers of ODT and deprotonated MUA are spontaneously incorporated into vesicles formed from 30:70 mixtures of cationic cetyltrimethylammonium tosylate (CTAT) and anionic sodium dodecyl benzenesulfonate (SDBS) surfactants. (b) Cryo-TEM image showing colocalization of AuMUA/ODT NPs with surfactant vesicles in aqueous solution. The amphiphilic NPs interact with the hydrophobic core of the vesicle walls (see the text) under basic conditions (pH 11) with 100 mM added tetramethylammonium chloride (TMACl).

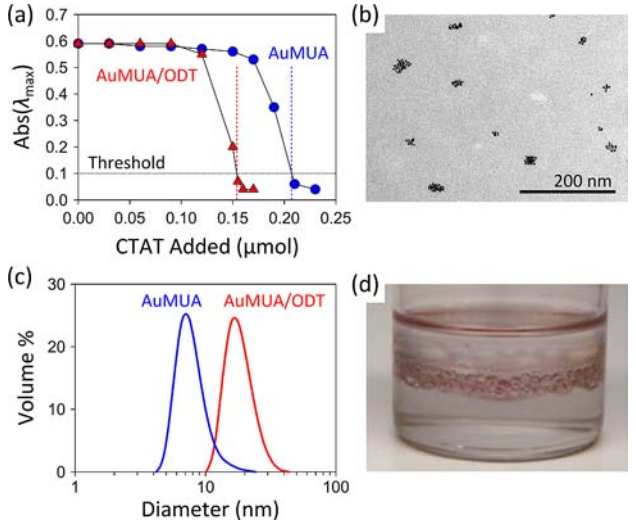

Figure 2. (a) Electrostatic titrations were used to quantify the fraction of charged MUA ligands on the surface of the AuMUA/ODT NPs. (b, c) AuMUA/ODT NPs form stable clusters of ~10 NPs in water (pH 11), as revealed by (b) TEM and (c) DLS. (d) Water-soluble AuMUA/ODT NPs accumulate at the water–toluene interface.

solution of AuMUA/ODT NPs (on a gold atom basis) caused the particles to precipitate sharply at the point of overall charge neutrality as monitored by UV–vis spectroscopy. By comparing the precipitation point of AuMUA/ODT NPs to that of analogous AuMUA particles, we determined the fraction of the NP surface covered with negatively charged MUA ligands (f); the desired surface ratio is given by $\chi_{surf} = (1 - f)/f$. For the NPs described here, $f \approx 0.74$ ($\chi_{surf} \approx 0.35$), indicating that ~26% of the NP surface was covered with hydrophobic ODT ligands. This ligand composition was further supported by ^{1}H NMR analysis of the amphiphilic NPs (see section 3 in the SI). Further increasing the amount of ODT (i.e., $\chi > 8$) caused the particles to precipitate from solution.

Even in the absence of visible precipitation, the amphiphilic AuMUA/ODT NPs interact in solution to form small NP clusters, as evidenced by transmission electron microscopy (TEM) and dynamic light scattering (DLS) (Figure 2b,c). The average size of the clusters was measured to be ~10 NPs by TEM and ~18 nm by DLS. By contrast, purely hydrophilic, negatively charged AuMUA NPs showed no signs of aggregation or cluster formation (see section 2 in the SI). The assembly of AuMUA/ODT NPs into stable clusters is likely driven by hydrophobic interactions between the ODT ligands, which concentrate within the cores of the clusters to reduce the number of energetically unfavorable ODT–water contacts. Similar micellar structures have been observed previously for amphiphilic NPs in water.[27,28] Repulsive electrostatic interactions between the negatively charged clusters prevented their further aggregation. The ζ potential of the NP clusters was measured to be -65 ± 15 mV (see section 4 in the SI).

It is important to note that the MUA and ODT ligands are not bound irreversibly to the gold surface but can redistribute[18] themselves dynamically in response to environmental changes. This is illustrated in Figure 2d, which shows how water-soluble AuMUA/ODT NPs migrate rapidly to the water–toluene interface upon vigorous agitation. As we[18] and others[19] have shown, the hydrophilic MUA ligands become enriched on the water side while the hydrophobic ODT ligands are enriched on the toluene side to reduce the total interfacial energy. We expect these labile ligands to redistribute themselves in a similar fashion upon incorporation into the bilayer structure of the vesicles.

Independent of the amphiphilic NPs, vesicles were prepared from a mixture of the cationic surfactant CTAT and the anionic surfactant sodium dodecyl benzenesulfonate (SDBS).[21,22,29] Surfactant vesicles were chosen over analogous lipid vesicles both for their stability at high pH (needed to deprotonate the MUA ligands) and for the simplicity of their preparation. Briefly, the two surfactants (30:70 w/w CTAT/SDBS) were added to deionized water to 1 wt % and agitated vigorously by vortex mixing until the mixture became homogeneous with a bluish hue. The resulting vesicles were polydisperse with diameters ranging from 50 to 150 nm as revealed by DLS and cryo-TEM. Most of the vesicles had one bilayer; however, some with two or three bilayers were observed by cryo-TEM. The bilayer thickness was measured previously by small-angle neutron scattering (SANS) to be ~2.5 nm.[21,22] Because of the excess amount of negatively charged SDBS, the ζ potential of the vesicles was negative and equal to -123 ± 14 mV.

The NP–vesicle structures shown in Figure 1b were prepared simply by mixing a solution of the functionalized AuMUA/ODT NPs with a solution containing the preformed surfactant vesicles (Figure 3a). Specifically, 1 mL of 1 wt % surfactant vesicle solution was added to 1 mL of 1 mM AuMUA/ODT solution, and the pH was adjusted to ~11 by addition of TMAOH; this was followed by vortex mixing for 5 min. To mitigate the repulsive electrostatic interactions between the NPs and the vesicles (see below), tetramethylammonium chloride (TMACl) was added to achieve an ionic strength of 100 mM, and the mixture was vortex-mixed for an

dx.doi.org/10.1021/ja400225n | J. Am. Chem. Soc. 2013, 135, 5950–5953

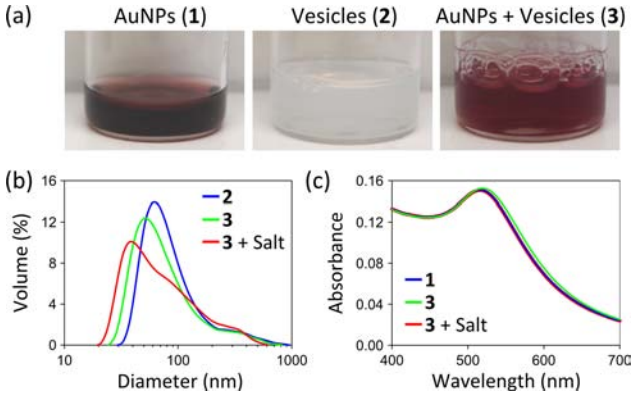

Figure 3. (a) Solutions of AuMUA/ODT (**1**) and surfactant vesicles (**2**) are simply mixed to form NP–vesicle structures (**3**). (b) Size distributions obtained by DLS for **2**, **3**, and **3** with 100 mM TMACl. (c) UV–vis extinction spectra for **1**, **3**, and **3** with 100 mM TMACl.

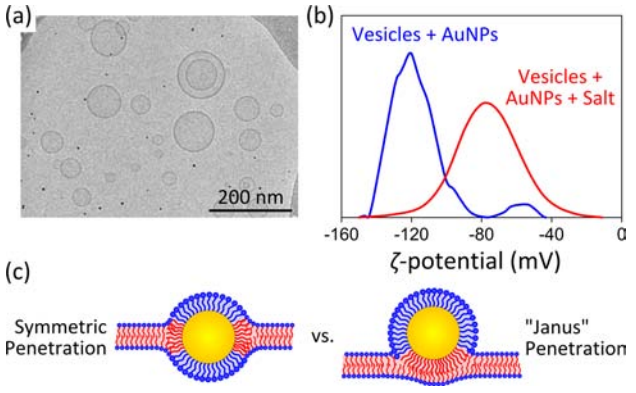

Figure 4. (a) Mixtures of vesicles and AuMUA/ODT NPs without added salt show no signs of NP–vesicle association by cryo-TEM. (b) ζ-potential distributions for mixtures of vesicles and AuMUA/ODT NPs with and without added salt. (c) Schematic illustrations of possible NP–vesicle configurations.

additional 10 min. Visually, the final solution appeared slightly turbid because of light scattering by the vesicles and wine-red as a result of absorption by the NPs at the surface plasmon resonance (SPR) wavelength (~520 nm).

The NP–vesicle mixtures with added salt were stable for more than 1 year without any precipitation. Furthermore, the addition of amphiphilic AuMUA/ODT NPs and salt did not significantly affect the size distribution of the surfactant vesicles as quantified by DLS (Figure 3b). This result suggests that the vesicle structures are not significantly disrupted by the amphiphilic particles and that they do not aggregate upon addition of salt. Similarly, the UV–vis extinction spectrum of the NP–vesicle structures showed little change from that of the initial NP solutions (Figure 3c). The lack of a red shift in the SPR peak suggests that the NPs remain well-dispersed from one another.[30]

To investigate the hypothesized association between amphiphilic AuMUA/ODT NPs and surfactant vesicles, we used cryo-TEM[31] to visualize the relative locations of NPs and vesicles frozen in solution at a particular instant in time. As shown in Figure 1b, all of the NPs in the field of view were colocalized with surfactant vesicles. This result is highly unlikely to occur by chance in the absence of attractive interactions between the NPs and the vesicles. The probability (p value) of obtaining these results assuming that the nanoparticles were distributed at random throughout the image is $\sim 10^{-11}$ (see section 5 in the SI). Therefore, we conclude that AuMUA/ODT NPs associate strongly with surfactant vesicles to form stable NP–vesicle complexes.

Importantly, *both* the hydrophilic MUA ligands and the hydrophobic ODT ligands were necessary to observe such NP–vesicle structures. To show this, we performed control experiments on analogous mixtures containing either AuMUA NPs or AuODT NPs. Mixtures of AuODT NPs and surfactant vesicles resulted in the rapid precipitation of the hydrophobic NPs from solution. By contrast, AuMUA NPs formed stable mixtures with surfactant vesicles but showed no association between the NPs and the vesicles under cryo-TEM (p value ≈ 0.7).

Additionally, NP–vesicle structures did not form in the absence of added salt, as evidenced by cryo-TEM (Figure 4a). The few instances of NP–vesicle colocalization observed are consistent with expectations based on a random (uniform) distribution of NPs throughout the field of view (p value ≈ 0.7). The lack of NP–vesicle association at low salt concentrations is further supported by ζ-potential measurements on mixtures of surfactant vesicles and AuMUA/ODT NPs with and without added TMACl (Figure 4b). Specifically, distributions of the ζ potential for NP–vesicle mixtures without salt showed two peaks, one near −120 mV (close to that for the vesicles alone, $\zeta = -123 \pm 14$ mV) and another near −60 mV (close to that for AuMUA/ODT NPs alone, $\zeta = -65 \pm 15$ mV). After the addition of 100 mM TMACl, distributions of the ζ potential contained just one peak near −80 mV, close to that of the vesicles alone in the presence of salt (-76 ± 13 mV). These results are consistent with the cryo-TEM observations and suggest that the NPs remain separate from the vesicles at lower salt concentrations ($c_s \approx 10$ mM due to counterions from the ionic surfactants; Figure 4a) but associate at higher salt concentrations ($c_s \approx 100$ mM; Figure 1a).

Physically, the addition of salt acts to decrease both the magnitude and the range of the repulsive electrostatic interactions between the negatively charged NPs and the like-charged vesicles.[10] In particular, the Debye screening length, which is characteristic of the range of electrostatic interactions, decreases from ~4 nm at low salt concentrations to ~1 nm at high salt concentrations. Consequently, under low-salt conditions, repulsive electrostatic forces maintain sufficient distance between the NPs and the bilayer surface as to prevent hydrophobic interactions between the ODT ligands and the bilayer core. Under high-salt conditions, however, the range of electrostatic interactions becomes comparable to the length of the ODT ligands, allowing the ligands to interact with the bilayer to guide the formation of NP–vesicle complexes.

Even with added salt, the NPs and vesicles remain negatively charged ($\zeta = -51 \pm 16$ mV and -76 ± 13 mV, respectively), and the NP–vesicle association is attributed solely to hydrophobic interactions between the ODT ligands and the bilayer core. The need for both hydrophilic and hydrophobic ligands suggests that some parts of the NP surface interact with the hydrophobic core of the bilayer while other parts remain in contact with the aqueous solution.

In the terminology of ref 20, it is unclear whether to classify the interaction as symmetric penetration or asymmetric ("Janus") penetration (Figure 4c). On the basis of simulations and theory,[20] the latter is preferred when repulsive interactions *within* the monolayer (i.e., between MUA and ODT) are strong

dx.doi.org/10.1021/ja400225n | J. Am. Chem. Soc. 2013, 135, 5950–5953

enough to induce spontaneous phase separation of the two ligands. Additionally, mobile ligands can segregate in response to the particles' local environment (e.g., a liquid interface,[18,19] an NP cluster, or a bilayer structure). In experiments, it is difficult to separate these two contributions. For example, does spontaneous phase separation of MUA and ODT on the NP surface drive the formation of NP−vesicle complexes *or* is phase separation induced by the change in ligand environment accompanying complex formation? Answering such questions will require further understanding of hierarchical assembly processes in which organization at one "level" (e.g., ligand segregation) is coupled to that at a higher "level" (e.g., NP−vesicle complex formation). The amphiphilic NPs described here should provide a useful model system for the study of such multiscale assembly processes. Furthermore, our results support a general strategy for the simple preparation of NP−bilayer complexes using adaptive surface chemistries that reconfigure in response to environmental cues. We are currently working to extend this concept to other NP materials (e.g., magnetic cobalt ferrite) and bilayer structures (e.g., lipids).

■ ASSOCIATED CONTENT

Supporting Information

Experimental details, TEM characterization of Au NPs, ligand composition as determined by ^{1}H NMR analysis, data from ζ-potential measurements, and analysis of cryo-TEM images. This material is available free of charge via the Internet at http://pubs.acs.org.

■ AUTHOR INFORMATION

Corresponding Author

kjmbishop@engr.psu.edu

Notes

The authors declare no competing financial interest.

■ ACKNOWLEDGMENTS

This work was supported by the Penn State MRSEC (NSF DMR-0820404). D.D. acknowledges partial support by the Russell Berrie Nanotechnology Institute.

■ REFERENCES

(1) Gopalakrishnan, G.; Danelon, C.; Izewska, P.; Prummer, M.; Bolinger, P. Y.; Geissbuhler, I.; Demurtas, D.; Dubochet, J.; Vogel, H. *Angew. Chem., Int. Ed.* **2006**, *45*, 5478.
(2) Kennedy, L. C.; Bickford, L. R.; Lewinski, N. A.; Coughlin, A. J.; Hu, Y.; Day, E. S.; West, J. L.; Drezek, R. A. *Small* **2011**, *7*, 169.
(3) Amstad, E.; Kohlbrecher, J.; Muller, E.; Schweizer, T.; Textor, M.; Reimhult, E. *Nano Lett.* **2011**, *11*, 1664.
(4) Chen, Y. J.; Bose, A.; Bothun, G. D. *ACS Nano* **2010**, *4*, 3215.
(5) Volodkin, D. V.; Skirtach, A. G.; Mohwald, H. *Angew. Chem., Int. Ed.* **2009**, *48*, 1807.
(6) Wu, G.; Mikhailovsky, A.; Khant, H. A.; Fu, C.; Chiu, W.; Zasadzinski, J. A. *J. Am. Chem. Soc.* **2008**, *130*, 8175.
(7) Michalet, X.; Pinaud, F. F.; Bentolila, L. A.; Tsay, J. M.; Doose, S.; Li, J. J.; Sundaresan, G.; Wu, A. M.; Gambhir, S. S.; Weiss, S. *Science* **2005**, *307*, 538.
(8) Kelly, K. L.; Coronado, E.; Zhao, L. L.; Schatz, G. C. *J. Phys. Chem. B* **2003**, *107*, 668.
(9) Blanton, S. A.; Hines, M. A.; Guyot-Sionnest, P. *Appl. Phys. Lett.* **1996**, *69*, 3905.
(10) Bishop, K. J. M.; Wilmer, C. E.; Soh, S.; Grzybowski, B. A. *Small* **2009**, *5*, 1600.
(11) Balgavy, P.; Dubnickova, M.; Kucerka, N.; Kiselev, M. A.; Yaradaikin, S. P.; Uhrikova, D. *Biochem. Biophys. Acta.* **2001**, *1512*, 40.
(12) Rasch, M. R.; Rossinyol, E.; Hueso, J. L.; Goodfellow, B. W.; Arbiol, J.; Korgel, B. A. *Nano Lett.* **2010**, *10*, 3733.
(13) He, J.; Liu, Y. J.; Babu, T.; Wei, Z. J.; Nie, Z. H. *J. Am. Chem. Soc.* **2012**, *134*, 11342.
(14) Dubertret, B.; Skourides, P.; Norris, D. J.; Noireaux, V.; Brivanlou, A. H.; Libchaber, A. *Science* **2002**, *298*, 1759.
(15) Ginzburg, V. V.; Balijepailli, S. *Nano Lett.* **2007**, *7*, 3716.
(16) Wi, H. S.; Lee, K.; Pak, H. K. *J. Phys.: Condens. Matter* **2008**, *20*, No. 494211.
(17) Verma, A.; Uzun, O.; Hu, Y. H.; Hu, Y.; Han, H. S.; Watson, N.; Chen, S. L.; Irvine, D. J.; Stellacci, F. *Nat. Mater.* **2008**, *7*, 588.
(18) Andala, D. M.; Shin, S. H. R.; Lee, H. Y.; Bishop, K. J. M. *ACS Nano* **2012**, *6*, 1044.
(19) Norgaard, K.; Weygand, M. J.; Kjaer, K.; Brust, M.; Bjornholm, T. *Faraday Discuss.* **2004**, *125*, 221.
(20) Van Lehn, R. C.; Alexander-Katz, A. *Soft Matter* **2011**, *7*, 11392.
(21) Lee, J.-H.; Gustin, J. P.; Chen, T.; Payne, G. F.; Raghavan, S. R. *Langmuir* **2005**, *21*, 26.
(22) Lee, J.-H.; Agarwal, V.; Bose, A.; Payne, G. F.; Raghavan, S. R. *Phys. Rev. Lett.* **2006**, *96*, No. 048102.
(23) Jana, N. R.; Peng, X. G. *J. Am. Chem. Soc.* **2003**, *125*, 14280.
(24) Kalsin, A. M.; Fialkowski, M.; Paszewski, M.; Smoukov, S. K.; Bishop, K. J. M.; Grzybowski, B. A. *Science* **2006**, *312*, 420.
(25) Wang, D. W.; Nap, R. J.; Lagzi, I.; Kowalczyk, B.; Han, S. B.; Grzybowski, B. A.; Szleifer, I. *J. Am. Chem. Soc.* **2011**, *133*, 2192.
(26) Kalsin, A. M.; Kowalczyk, B.; Wesson, P.; Paszewski, M.; Grzybowski, B. A. *J. Am. Chem. Soc.* **2007**, *129*, 6664.
(27) Chen, Q.; Whitmer, J. K.; Jiang, S.; Bae, S. C.; Luijten, E.; Granick, S. *Science* **2011**, *331*, 199.
(28) Larson-Smith, K.; Pozzo, D. C. *Soft Matter* **2011**, *7*, 5339.
(29) Kaler, E. W.; Murthy, A. K.; Rodriguez, B. E.; Zasadzinski, J. A. *Science* **1989**, *245*, 1371.
(30) Ghosh, S. K.; Pal, T. *Chem. Rev.* **2007**, *107*, 4797.
(31) Danino, D. *Curr. Opin. Colloid Interface Sci.* **2012**, *17*, 316.